Electrical, morphological, thermal and mechanical properties of low density polyethylene/zinc oxide nanocomposites prepared by melt mixing method

HALE BERBER YAMAK[a,*], MIHRIGUL ALTAN[b], AHMET ALTINDAL[c]
[a]*Department of Metallurgical and Materials Engineering, Yıldız Technical University, Istanbul, Turkey*
[b]*Department of Mechanical Engineering, Yıldız Technical University, Istanbul, Turkey*
[c]*Department of Physics, Yıldız Technical University, Istanbul, Turkey*

In this study, low density polyethylene/zinc oxide (LDPE/ZnO) nanocomposites were prepared at different concentrations of ZnO nanoparticles, ranged from 0 to 36 wt%, by melt mixing method using twin-screw extruder in order to investigate the effect of presence and concentration change of nano-sized ZnO particles on the impedance spectra of LDPE and also on mechanical, thermal and morphological properties. Then, nanocomposite films with 170 micron thickness were obtained from the granulated nanocomposites by two-roll mills and hot pressing, respectively. Electrical properties of pure LDPE and LDPE/ZnO nanocomposite films were studied by impedance measurements over a temperature range of 298–400 K and in the frequency range from 50 Hz to 10 MHz. The room temperature conductivity evaluated from the straight-line fit in measured I-V plot and was found to be 1.3x10-5 S cm^{-1} and 4.7x10^{-3} S cm^{-1} for pure and 18% ZnO filled film, respectively. The results of impedance analysis showed that the inclusion of ZnO particles improved the dielectric properties of the samples. It was also observed that loss tangent increased as the frequency increased and reached a maximum and thereafter decreased. The thermal degradation temperatures of the LDPE showed an increase with presence and increasing content of the ZnO in LDPE. It was also determined that the tensile strength of the pure LDPE raised from 8.01 MPa to 8.60 MPa with the addition of ZnO nano particles but on the contrary, the elongation (%) of nanocomposites decreased apparently from 1.63 to 0.16.

(Received August 8, 2016; accepted November 25, 2016)

Keywords: Dielectric property, Polymer nanocomposite, Nano-sized ZnO, LDPE

1. Introduction

Polymer nanocomposites comprising embedded nano-sized inorganic filler into organic polymer matrix have an increasing attention due to further improve the mechanical, thermal, optic and electrical properties compared with conventional polymer composites [1-5]. Unlike the bulk materials and conventional micron sized fillers, the nano fillers having a smaller size, larger specific surface area and higher surface energy create excellent interfacial interactions on polymer branches that allow to obtain composites in better properties. The choice of the nano fillers in terms of the type, structure, shape, size and concentration is a significant parameter playing an essential role in the features and applications of the nanocomposites [6]. Previous researchers experienced many different inorganic nano materials to develop the electrical properties of the polymer composites. Carbon black [7,8] and graphite [9] are very common materials to increase the electrical properties of the polymers. In recent years, graphene is also very popular for its intended use [10-12]. Besides, zinc oxide (ZnO), as a functional nano-sized inorganic filler has gained great interest in developing polymer nanocomposites. Namely, a nanocomposite containing ZnO nanostructures can be obtained to use various applications including UV light-emitters, varistors, transparent high power electronics, surface acoustic wave devices, piezo-electric transducers, gas sensors and solar cells [13-19].

ZnO is an important and attractive semi conductive metal oxide with a wide band gap (3.37ev), large exciton binding energy (60 meV) at room temperature, n-type conductivity and high chemical stability. It is abundant in nature and environmentally friendly, and also shows a marked antibacterial activity without the presence of light. Moreover, nanostructured ZnO has exceptional piezoelectric, optical, electrical conductivity, mechanical, dielectric and microwave absorption properties [16-19]. It is possible to produce nanostructured ZnO in different morphologies such as nanoparticles, nanorods, nanosheets, nanowires, nanowhiskers, nanotubes and nanoflowers [19-25]. As well as the morphology, amount of added ZnO nanostructures and the type of polymer matrix also determine the performance of the obtained nanocomposite materials. ZnO nanostructures were combined with different type of polymers like polyurethane, epoxy resin, poly(methyl methacrylate), polystyrene, polyethylene, polypropylene, etc. [13-20, 25-28].

Among these polymers, low-density polyethylene (LDPE) is relatively preferred as a thermoplastic polymer matrix because of its good physical properties and mechanical capability, high breakdown strength, high

resistance to chemicals, low price and ease of processing. It has also very low electrical conductivity and poor dielectric properties [29-32]. Therefore, the combination of nano-sized ZnO with LDPE is usually performed in order to enhance the electrical properties of LDPE. There are some studies concerning the influence of nano-sized ZnO on electrical properties as well as mechanical and morphological properties of LDPE in the literature [27,31,33-35]. It could be possible to increase dielectric constant and mechanical strength, and to decrease electrical resistivity of LDPE by adding ZnO nanostructures depending on the volume fraction and shape of nano-sized ZnO, dispersion of the ZnO nanostructures in polymer matrix and preparation method.

In this study, in order to improve the electrical as well as mechanical properties of LDPE, we incorporated the ZnO nanoparticles into the LDPE matrix by continuous single-step extrusion process. This applied melt mixing method provides versatile advantages for the preparation of LDPE based nanocomposites compared with the other common methods involving in situ polymerization and solution mixing. Because, this method allows easy mixing and good dispersion of the nanofillers within the thermoplastic matrix, and also provides fast production with cost effective and environmentally friendly process, being solvent free [7, 27, 31, 36]. Also, the use of various compatibilizers is common in the melt mixing process of LDPE/ZnO nanocomposites in order to obtain the fine dispersions and facilitate the process. However, it was reported that such additives act to reduce the dielectric constants of the LDPE/ZnO nanocomposites compared to those prepared without compatibilizers [27,33]. Hence, the LDPE/ZnO nanocomposites were produced by twin-screw extruder without the use of auxiliary components in this study. In order to determine the effect of presence and also concentration change of ZnO nanoparticles on the dielectric, mechanical, thermal and morphological properties of LDPE, the LDPE/ZnO nanocomposites were prepared at different weight ratios of ZnO nanoparticles ranging from 0 to 36 wt% in granular form. After that, these granules were made into films by hot pressing to be used in analyzes. The dielectric properties such as dielectric constant and loss tangent of the LDPE/ZnO nanocomposite films containing different amounts of ZnO were studied with impedance analyzer. Also, mechanical tensile strengths, thermal stabilities, crystallinity degrees and morphologies of these films were investigated by using tensile test machine, thermogravimetric analyzer (TGA), differential scanning calorimetry (DSC) and scanning electron microscopy (SEM), respectively. All analysis results were discussed in detail, and a comparison was made between the pure LDPE and nanocomposites with different weight ratio of ZnO nanoparticles considering the literature.

2. Experimental

2.1. Materials

Commercial grade of low density polyethylene (LDPE), (PETILEN I22-19T) used as polymer matrix in this work was provided by Petkim Petrochemical Company (Turkey) in the forms of granule, with a melt index of 17-29 g/10 min by ASTM D1238 and a density of 0.917-0.921 g/cm^3 by D1505. The number-average molecular weight (Mn), weight-average molecular weight (Mw) and polydispersity index (PDI) values of LDPE were 29600, 157000 g.mol^{-1} and 5.3, respectively. The zinc oxide (ZnO) nano-sized particles (Nabond, Inc., China) had an average diameter of 20 nm. No solvents, modifiers, compatibilizers or processing aids were used.

2.2. Preparation of LDPE/ZnO Nanocomposites

The LDPE/ZnO nanocomposites were prepared by melt mixing method using twin-screw extruder with co-rotating, a screw diameter of 22 mm and a screw ratio of 40:1 length to diameter (Coperion Company). In nanocomposite preparation processes, a total amount of 500 grams consisting of LDPE granules and ZnO nano-powders was used. The ZnO nanoparticle content in this total amount was ranged from 0 to 36 wt%. Firstly, LDPE granules and ZnO nanoparticles were mixed mechanically at room temperature. Then, they were fed to the extruder at 250 rpm screw speed. The temperatures were set at 120 ^{o}C and 140 ^{o}C in feeding and barrel zones, respectively. End of the extrusion process, the LDPE/ZnO nanocomposite samples were obtained in the granule form. To form films from nanocomposite granules, 40 grams of these granules were first made melt using two-roll mills (LabTech Engineering Co. Inc.) which were set at 135 ^{o}C and at 35 rpm rotate speed, and then 2.5 grams of the melted samples were hot pressed at 130 ^{o}C under 16 MPa for 45 s into plates using LabTech hydraulic laboratory press. The nanocomposite films of 170 μm thickness were obtained.

2.3. Characterizations

Thermogravimetric analyses (TGA) were performed using a Rigaku Thermo plus EVO instrument under flowing nitrogen. Samples of 5–10 mg were heated from 25 to 600 °C at a heating rate of 10 °C/min.

Differential Scanning Calorimetry (DSC) analyses of the specimens were done in a Perkin Elmer DSC under flowing nitrogen. Specimens were placed in a sealed aluminum cells using a quantity 5-7 mg and heated from 25 to 200 °C at a rate of 10 °C/min. After isothermal conditions at 200 °C for 1 min, the samples were cooled down to 30 °C and reheated to 200 °C at a rate of 10 °C/min. The data obtained from the first cooling and second heating scans were used in order to determine the temperatures of melting, as well as melting and crystallization enthalpies.

X-ray diffraction (XRD) analysis of the nano-sized ZnO, pure LDPE and LDPE/ZnO nanocomposites were studied by using a Philips Panalytical X'Pert-Pro diffractometer with a CuKα radiation (λ = 0.15418 nm) operated at 45 kV and 40 mA. The scanning was done in the region of 2θ from 20° to 80°.

Morphology of the nano-sized pure ZnO, pure LDPE and each polymer nanocomposite film having different ZnO contetnt were investigated by Scanning Electron Microscopy, SEM (JEOL JSM-5910 LV). The fracture surfaces of the films were obtained by keeping them in liquid nitrogen for 10 seconds. Then, they were broken and the fractured surfaces were coated with gold prior SEM analysis.

The dielectric measurements were carried out in the frequency range from 50 Hz to 10 MHz and temperature between 298 – 400 K, using an impedance analyzer (HP, Model 4292) equipped with a four-terminal test fixture. Au-LDPE-Au capacitive devices were fabricated in a sandwich configuration with an active conduction area of 7.8×10^{-6} m^2. The circular Au contacts on the LDPE surfaces were formed by thermal evaporation of Au at pressure of approximately 1.0×10^{-5} mbar using an Edwards Auto 500 thermal evaporator system. Impedance spectroscopy was employed to determine the frequency-dependent transport behavior of the samples. The temperature of each sample was determined during the measurements using a pre-calibrated K-type thermocouple with an error of ± 0.1 K. All measurements were performed under vacuum ($\leq 10^{-3}$ mbar) and in the dark, but the values did not changed under illumination with the indoor lighting. Impedance data were recorded using an IEEE-488 data acquisition system incorporated to a personnel computer.

The tensile properties of the pure LDPE and ZnO nanoparticles incorporated LDPE films were determined using an INSTRON 3369 Universal testing machine with 1 kN load cell at a crosshead speed of 100 mm/min. The tensile strength tests were performed with the bone type test specimens in dimensions of 96×10×0.24 mm at atmospheric conditions. For each film, three specimens were used and then the average result was reported.

The density tests of the LDPE/ZnO nanocomposites were done using Mettler Toledo's Density Kits mounted on Mettler Toledo NewClassic ML Balance at atmospheric conditions and accurately applied by three decimal results.

3. Results and discussion

3.1. Thermal properties

The thermal stability of LDPE matrix depending on the amount of zinc oxide in the composite was examined by Thermogravimetric Analyzer (TGA). The TGA curves for the pure LDPE and the nanocomposites (LDPE/ZnO) are shown in Fig. 1 (a) as a function of % weight loss with the increase in temperature. The thermograms of all the samples demonstrated only one discrete weight loss step in the temperature range of 400-500 ^oC, corresponding to the decomposition of LDPE in nitrogen atmosphere. For an easy comparison, we focused on a narrow range of weight loss (2-10%) extracted from the TGA curves, as shown on the Fig. 1 (b). In addition, the onset and peak degradation temperatures were calculated from the 1st derivative of the weight loss curves and given in Table 1. The onset and peak degradation temperatures were respectively 417.98 ^oC and 490.70 ^oC for pure LDPE. By loading of the nano-sized ZnO into the polymer matrix, these values were varied depending on the ZnO content in the composites, as shown Table 1. They were not affected too much by the low amount of ZnO. On the other hand, it was detected to shift to higher peak degradation temperatures at high amount of ZnO, especially over 24 wt% ZnO. According to the TGA curves and the degradation temperatures values, it can be said that the thermal stability of LDPE is enhanced by the nano-sized ZnO over a certain amount. The nanoparticles of ZnO in the LDPE matrix can limit the thermal motion of polymer chains and act as thermal insulator and mass transport barrier against the volatile products generated during decomposition. This results in LDPE chains starting to decompose at higher temperatures [13, 37]. Also, it was found that the total mass loss values of the composites were in good agreement with the amount of ZnO initially loaded into the LDPE matrix.

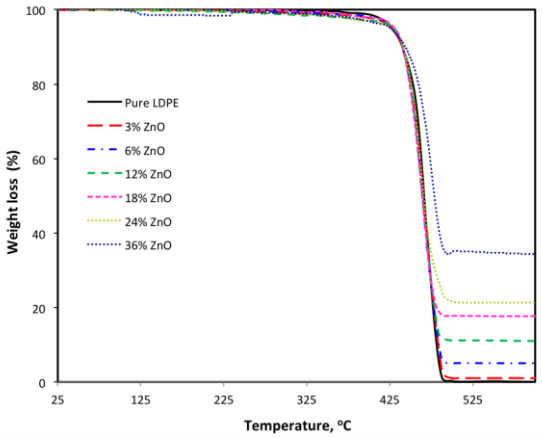

(a)

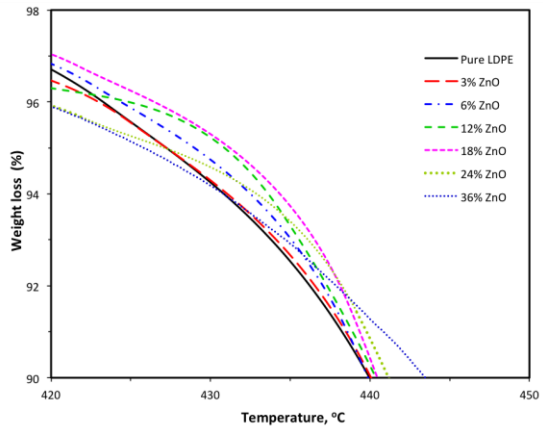

(b)

Fig. 1. TGA curves, (a) and (b), for pure LDPE and LDPE/ZnO nanocomposites

The melting behavior, enthalpy changes and crystallinity of the pure LDPE and the LDPE/ZnO nanocomposites were investigated by Differential Scanning Calorimetery (DSC). Melting and crystallization curves from second heating and first cooling cycles for all the samples are given in Fig. 2 and Fig. 3. The peak

melting temperature (T_m), melting and crystallization enthalpies (ΔH_m and ΔH_c), and percent crystallinity (X_c) are listed in Table 1. X_c of LDPE phase was calculated using the Eq. (1);

$$X_c = (\Delta H_m - \Delta H_c)/\Delta H_m^{\circ} \times 100 \quad (1)$$

where ΔH^o_m, the heat of melting for 100% crystalline PE was taken to be 293 J g^{-1} [38].

As seen from Fig. 2 and Table 1, the presence and increasing amount of ZnO nano particles did not significant influence on the T_m of LDPE. With increasing ZnO content in the LDPE matrix, T_m slightly shifted to a lower temperature. For example, T_m was observed at 107.09 ^oC for pure LDPE, while only about 1 °C decrease in melting temperature of the LDPE occurred for composite containing the highest amount of ZnO (36 wt% ZnO). Also the T_c slightly shifted to higher values with increasing ZnO content (as seen in Fig. 3). When we focused on the melting and crystallization curves, and their enthalpy data from Table 1, ΔH_m, ΔH_c and X_c values were found to increase with the addition of ZnO up to 12 wt%, as compared to pure LDPE, and then started to decrease with this amount was exceeded. Especially for over 24 wt% ZnO content, these thermal values fell below that of the pure LDPE, and this effect was more evident. It is generally believed that nano fillers can make two different effects as the nucleating and the retarding on the non-isothermal polymer matrix crystallization, there is a compromise between the nucleating and the retarding effects [39]. Increased crystallinity at low ZnO content, it can be explained by the ZnO nanoparticles act as nucleating agents in polymer crystallization and the X_C increases slightly by the incorporation of ZnO nanoparticles, from 27.30% for LDPE to 33.96% for the nanocomposite with 6 wt% ZnO content. On the other hand, the observed gradual decrease in crystallinity can be due to the retarding effect of the nanoparticles whose amounts in composite were above 6 wt%. At high ZnO content, the formation of particle aggregates occurs and the aggregation will increase with increasing content of nanoparticles in the composite. Hence, this results in inhibition of the crystallization and smaller X_c. [13,30,40]. The SEM micrographs of LDPE/ZnO nanocomposites also confirms these results obtained from DSC for high contents of ZnO.

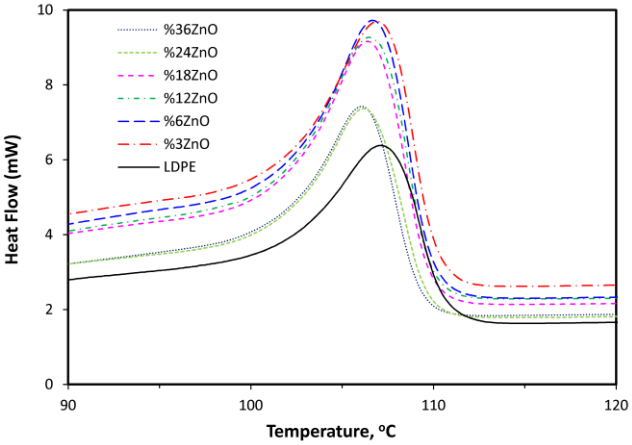

Fig. 2. DSC melting curves for pure LDPE and LDPE/ZnO nanocomposites

Table 1. Thermal data from TGA and DSC of the pure LDPE and ZnO /LDPE nanocomposites at different ZnO content

Specimen	$T_{o,d}$ ^oC	$T_{p,d}$ ^oC	$T_{m,}$ ^oC	$\Delta H_{m,}$ J/g	$\Delta H_{c,}$ J/g	X_c
LDPE	417.98	490.70	107.09	30.7596	-49.2283	27.30
LDPE 3% ZnO	411.17	488.59	106.85	35.0813	-56.6181	31.30
LDPE 6% ZnO	415.43	488.84	106.69	38.2775	-61.2412	33.96
LDPE 12% ZnO	391.63	484.58	106.53	34.0761	-54.6263	30.27
LDPE 18% ZnO	397.34	485.43	106.36	32.7375	-50.5157	28.41
LDPE 24% ZnO	401.60	491.90	106.23	29.1594	-45.6093	25.52
LDPE 36% ZnO	413.13	497.89	106.07	23.5482	-39.9009	21.65

$T_{o,d}$:onset degradation temperature; $T_{p,d}$:peak degradation temperature; T_m :melting temperature;
ΔH_m :melting enthalpy; ΔH_c :crystallization enthalpy; X_c :crystallinity percentage

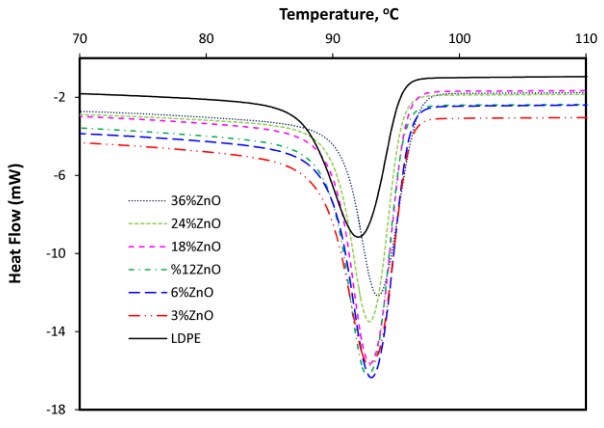

Fig. 3. DSC crystallization curves for pure LDPE and LDPE/ZnO nanocomposites

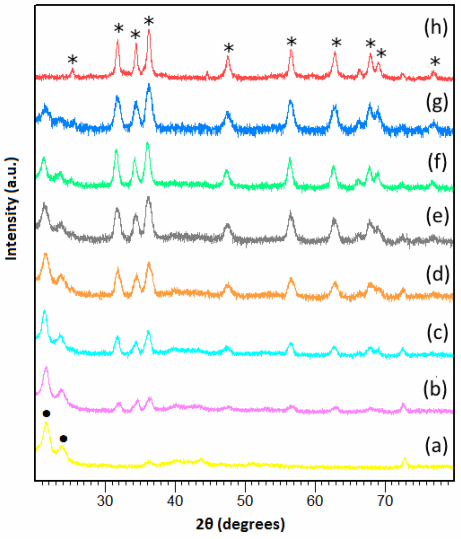

Fig. 4. XRD patterns of LDPE (a), ZnO (h) and LDPE/ZnO nanocomposites containing 3 wt% (b), 6 wt% (c), 12 wt% (d), 18 wt% (e), 24 wt% (f), 36 wt% (g) of ZnO content

3.2. X-ray diffraction

Fig. 4 shows the XRD patterns of the ZnO nanoparticles, pure LDPE and LDPE/ZnO nanocomposites with different ZnO loading. Two typical diffraction peaks were observed at 21.62^o and 23.98^o for the LDPE. They respectively indicate the crystallographic planes (110) and (200) of the orthorhombic form of polyethylene superimposed on the amorphous halo [41]. For the ZnO nano-powder, the characteristic peaks were detected at 31.82^o, 34.43^o, 36.29^o, 47.47^o, 56.58^o, 62.90^o and 67.86^o. When the XRD patterns of the LDPE/ZnO nanocomposites compared with that of LDPE and ZnO, the typical diffraction peaks of both LDPE and ZnO were also seen for the composites. The intensities of ZnO peaks increased with increasing ZnO content in the composite. The characteristic peaks of LDPE at 21.62^o and 23.98^o did not change, and a decrease in its peak intensities was observed depending on increasing amount of ZnO. Moreover, no new diffraction peak was seen for the LDPE/ZnO composites. All these results indicate that there are no new-formed chemical bonds, and instead the physical interactions may occur between the ZnO nano-particles and the LDPE matrix during the extrusion process. Also, it can be said that the loading of nano-sized ZnO to the polymer matrix does not have any significant effect on the main LDPE crystalline structure. However, the crystallinity degree of LDPE may be affected by the presence of the ZnO particles and the physical interactions between them. The variation in the intensities of LDPE and ZnO diffraction peaks and the DSC results support this inference.

3.3. Morphology

The SEM images of the nano-sized pure ZnO, pure LDPE and composite films are given in Fig. 5. It is apparent that agglomerations in the matrix increases, as the particle content increases. In the case of the absence of the organic filler, as seen in SEM image of pure LDPE, the fracture surface shows great plastic deformation. On the other hand, particle included composites gave less deformed surfaces plastically due to the harder structure of nano ZnO than polymer itself. While 3, 6, 12 wt% concentrations were more successful in terms of particle distribution, over 12 wt% particle content, many particles were did not embed in the matrix. At these high concentrations of ZnO, the particles could not make an interaction with LDPE and could not be wetted by the matrix. Consequently, the extrusion process, which was carried out without using any compatibilizers, allowed good dispersions of ZnO nanoparticles in the LDPE matrix up to 12 wt%. Over this amounts of ZnO nanoparticles, the use of a compound as compatibilizer can be needed in order to obtain LDPE/ZnO nanocomposites having fine dispersions [33].

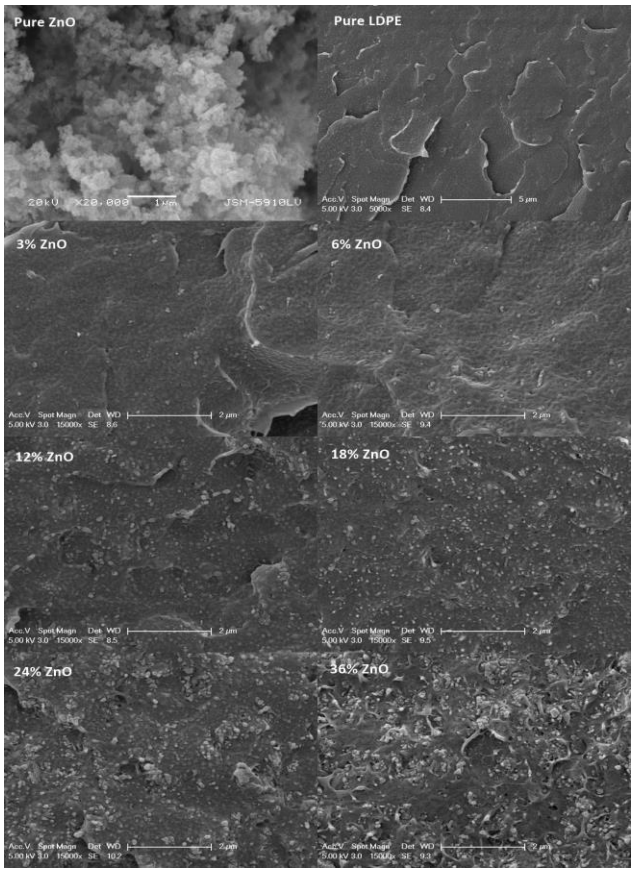

Fig. 5. SEM images of pure ZnO, pure LDPE and LDPE/ZnO nanocomposites containing 3 wt%, 6 wt%, 12 wt%, 18 wt%, 24 wt%, 36 wt% of ZnO content

3.4. Impedance spectroscopy

The impedance spectra of the LDPE/ZnO samples were systematically measured in the frequency range of 100 - 10 × 10^6 Hz for all samples at different fixed temperatures.

The complex impedance, Z*(ω) is given in Eq. (2);

$$Z^*(\omega) = R(\omega) + jX(\omega) \qquad (2)$$

where R(ω) and X(ω) are the real and imaginary parts of impedance. Fig. 6 (a) and (b) shows the frequency dependence of the real and imaginary parts of the measured impedance for LDPE and LDPE/ZnO at room temperature, respectively.

It becomes clear that from the Fig. 6 (a) that the magnitude of R(ω) decreases with the increase of both ZnO content and frequency at low frequencies. At higher frequency the value of R(ω) merges irrespective of ZnO content. The curves also display the single relaxation process and the decrease in real part of the complex impedance indicates an increase in ac conductivity with ZnO content. The decrease in real part of the complex impedance with increasing ZnO loading can be attributed to the increase of free charge carriers accumulation in the polymer. This may reduce the inter-particle distance of nanofiller and decrease the charge trapping sites. It is clearly seen from SEM images of the sample the inter-particle distance of nano filler is decreased. Hence, the decrease in resistivity is related to inter-particle distance in the polymer. The imaginary part of the complex impedance, X(ω), increased with frequency for all the ZnO content ranges studied here, attaining a maximum value X_{max} and, thereafter, decreased. The frequency dependence of the imaginary part of impedance indicates that the frequency at which X_{max} occurred, called the relaxation frequency, shifted to higher frequency regions as the ZnO content increased as shown in Fig. 6 (b). The appearance of peak in the loss spectrum and maximum shifts to higher frequency suggests the existence of relaxation properties of the material. The asymmetric broadening of the peaks on increasing ZnO content confirms the electrical processes in the material with a spread of relaxation time [42]. Further, all the curves merge at higher frequency irrespective of ZnO content. The relaxation phenomenon in the material may be due to the presence of immobile species/defects.

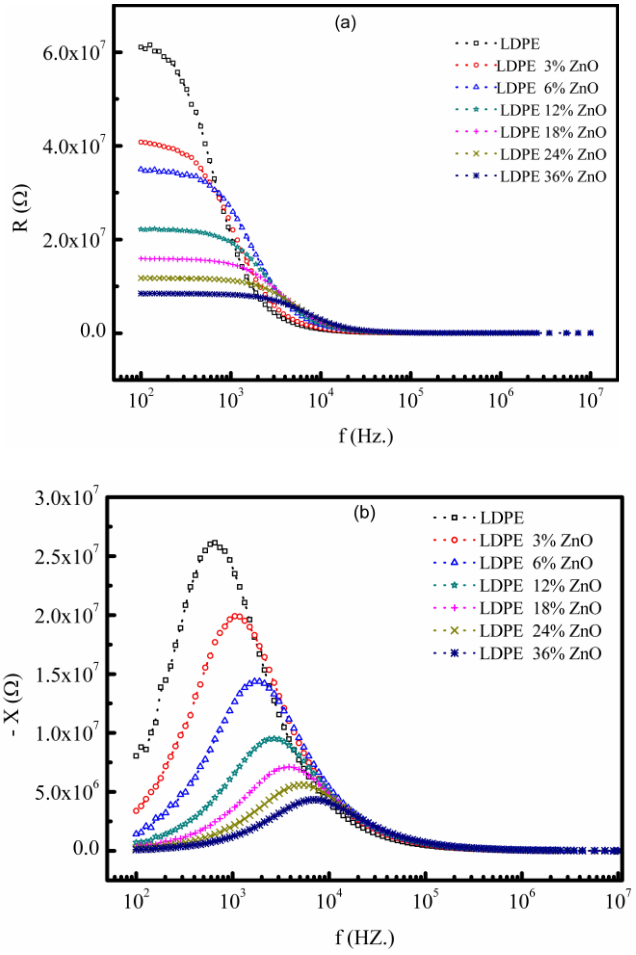

Fig. 6. Frequency dependence of the real (a) and imaginary (b) parts of impedance at room temperature for LDPE and LDPE/ZnO

Cole–cole spectra of the complex impedance, $Z^*(\omega)$ of the samples were recorded in the frequency range of 100 - 10× 10^6 Hz. Fig. 7 shows the measured complex impedance spectra (Cole–Cole plot) for LDPE at indicated temperatures. The measured impedance spectrum of LDPE is characterized by the appearance of semicircular arcs whose pattern, contrary to its shape, changes when the temperature is increased. Such a pattern tells us about the electrical processes occurring within the sample and their correlation with the sample microstructure when modelled in terms of an electrical equivalent circuit.

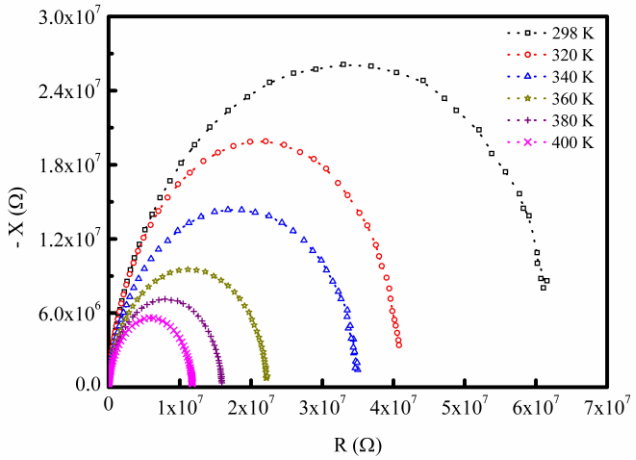

Fig. 7. Cole–Cole plot of the sample of LDPE at selected temperatures

An ideal semicircle in a complex plane plot appears only in the Debye dispersion relationship for a single relaxation time process. On the complex plane plot, only depressed semicircles with different radiuses were observed, indicating deviation from the Debye dispersion relationship. The depressed semicircles indicate that the maximum of the imaginary part of impedance is smaller than the half of the real part of impedance. The effect of temperature on the impedance spectra of the sample becomes clearly visible with a rise in temperature. In the case of a depressed semicircle in the impedance spectra, the relaxation time is considered as a distribution of values, rather than a single relaxation time. In this case, the measured impedance data can be modelled as a resistor (R_0) in parallel with a constant phase element (CPE) in series with another resistor (R_∞). The series resistance (R_∞) in the equivalent circuit represents the ohmic losses in the test fixture and electrode sheet resistance. The parallel resistance is of the test material. The presence of the constant phase element represents a slight distribution of relaxation times instead of a discrete relaxation time. This conclusion was supported by another type of Bode plot (log |Z| versus log |f|). It was found that the slope for log |Z| versus log |f| is between -0.48 and - 0.54 which indicates the presence of a CPE.

The measured complex impedance data were used to calculate the real (ε′(ω)), and imaginary (ε′′(ω)) parts of the complex dielectric function, ε*(ω) shown in Eq. (3).

$$\varepsilon^*(\omega) = \varepsilon'(\omega) - j\varepsilon''(\omega) \quad (3)$$

The relation between the dielectric function and the impedance can be given in Eq. (4) [43];

$$\varepsilon^*(\omega) = \frac{1}{j\omega C_0 Z^*(\omega)} = \varepsilon'(\omega) - j\varepsilon''(\omega) \quad (4)$$

where Z*(ω) is the measured impedance, C_0 is the capacitance of the empty measuring cell and ω is the angular frequency of the applied signal. Fig. 8 represents the frequency dependence of the real permittivity, ε′(ω), of the LDPE with various ZnO incorporation at room temperature. In all the cases, a strong frequency dispersion of permittivity, ε′(ω), is observed in the low frequency region followed by a nearly frequency independent behavior in the high frequency region. It is clear from the graphs that ε′(ω) decrease with increase in frequency, indicating a normal behavior of dielectric materials having mobile charge carriers, and thus become constant at higher frequencies. A reasonable explanation for the observed frequency dependence of ε′(ω) can be given by following the Koops's theory [35]. In this model the solid is assumed to be composed of well conducting grains separated by highly resistive thin layers, grain boundaries. As a consequence of the applied signal to the sample, a space charge polarization is built up at the grain boundaries. The induced space charge polarization is controlled by the available free charges on the grain boundary and the conductivity of the sample. According to this model, the main contribution to the dielectric constant at low frequencies comes from the grain boundaries, which have a high dielectric constant. On the other hand, at high frequencies, the dielectric behavior of the sample is dominated by the grains, which have a small dielectric constant.

As shown in Fig. 8, the real permittivity changes obtained depending on the frequency of the pure LDPE and all LDPE/ZnO nanocomposites exhibits the same behavior. Also, the increase in ε′(ω) by the incorporation of ZnO particles in LDPE matrix is clear. This is possibly due to the polar nature and low dielectric property of ZnO nanoparticles [35,44-45]. There is an additional aspect that should be recognized and accounted for in the interpretation of the high frequency behavior of ε′(ω). With the increase in frequency, at higher frequency, the variation in the field is too rapid for the dipoles to align themselves, so their contribution to the polarization and hence, to dielectric permittivity can become negligible as given in Fig. 8. These frequency-dependent permittivity behaviors of these films containing different amounts of ZnO nanoparticles, ranged from 0 to 36 wt%, is consistent with the previous literature on LDPE/ZnO nanocomposites. However, the obtained permittivity values were higher compared to the previously studies [13,27,33,46]. The permittivity depends directly on the system and process as well as the filler volume fraction. Therefore, many factors, such as physical conditions, applied sample preparation methods and properties of both filler and polymer matrix constituting a composite, have

significant influences on the permittivity [33,47-49].

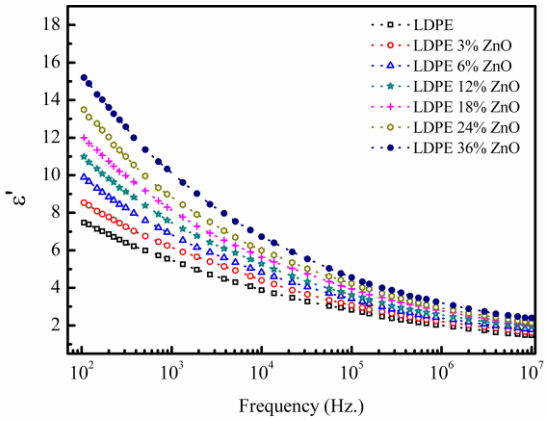

Fig. 8. Comparison of the real part of the complex dielectric function for LDPE and LDPE/ZnO at room temperature

Furthermore, it was found that the dielectric loss increases in is general as the filler contents and temperature increase. The increase in dielectric loss with the increase of filler contents can be attributed to the interfacial polarization. On the other hand, the increase of dielectric loss with temperature can be explained by conduction losses, vibration losses. At low temperature condition, losses are minimum as they depend on the ac resistivity and frequency. As the temperature increases, the ac resistivity increases and so the conduction losses increase.

The relation between the real and the imaginary parts of the complex dielectric function defined as loss tangent, tan δ given in Eq. (5).

$$tan\delta = \frac{\varepsilon'(\omega)}{\varepsilon''(\omega)} \quad (5)$$

For illustration, Fig. 9 shows the temperature and the frequency dependences of the loss tangent, tan δ, for the sample of LDPE 24 wt% ZnO. It is clear from the Fig. 9 that tan δ increases as the frequency increases and reaches a maximum at ω_{max} and thereafter decreases. As the temperature increases the frequency at which tan δ reaches a maximum shifted towards higher frequencies. The increase in tan δ in the low frequency range may be due to a contribution of the low-frequency relaxation process, as well as to dc conductivity in the examined sample. A same type of temperature and frequency dependence of tan δ with different ω_{max} and magnitude was observed for other samples investigated. It was observed that the tan δ increase with increase of ZnO content.

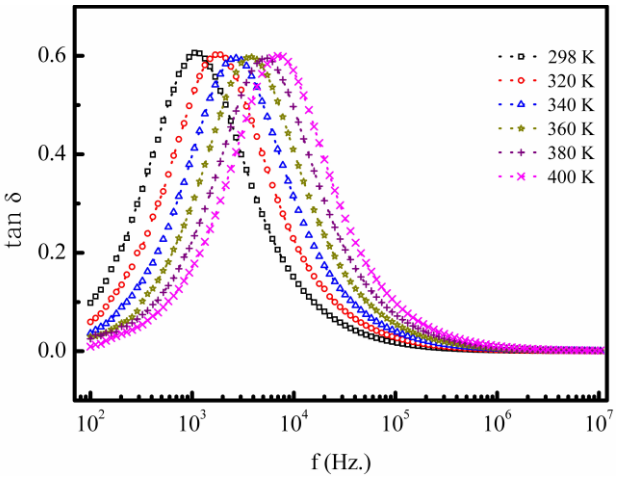

Fig. 9. Frequency dependence of tan δ for LDPE with 24% ZnO content at indicated temperatures

3.5. Mechanical properties

Tensile stress, young modulus and elongation at break of the composite films were reported in Table 2. The results showed that as the particle content increased, young modulus increased and elongation at break decreased due to the hardness of the particles. Moreover, the change in mechanical properties of the LDPE films depends on particle dispersion of nano ZnO particles. The presence of the well dispersion in the matrix provides good interfacial adhesion and this increased the ability of the interfacial structure to show higher elastic modulus and tensile strength. On the other hand, although the amount of particle content was increased from 3 wt% to 36 wt% within a systematic order, mechanical properties did not changed obviously. This is due to the agglomeration effect of the ZnO particles as verified in the SEM images of the films (Fig. 5). Inorganic nano particles tend to agglomerate more than micro particles [50,51]. The agglomerated particles induce stress concentration and they act as micro-cracks initiator and in this regard, high amount of particle concentration could not improve the mechanical properties. Furthermore, the high amount of particle concentration inhibits the flexibility of the molecular chain movement resulting in a more brittle structure with sharp decrease in elongation. As a result, up to 12 wt% of nano ZnO addition could be accepted as a threshold in improving the tensile strengths of the LDPE/ZnO nanocomposites. In addition to the mechanical tests, the density measurements were also performed and the results were given in Table 2. The density value of the pure polyethylene was 0.92. By the loading of nano-sized ZnO to the polymer matrix, it was observed an increase in the density of the polymer matrix, and this increase continued linearly with increasing ratio of ZnO in the nanocomposite. These density test results were compatible with increasing Young Modulus values of the composite films.

Table 2. Tensile properties and densities of the LDPE/ZnO composites

Specimen	Tensile stress (MPa)	Young Modulus (GPa)	Elongation at break (%)	Densities ($g.cm^{-1}$)
LDPE	8.01±0.20	0.13±0.01	1.63±0.26	0.92
LDPE 3% ZnO	8.60±0.26	0.16±0.01	1.39±0.37	0.93
LDPE 6% ZnO	8.51±0.34	0.17±0.02	0.96±0.18	0.95
LDPE 12 % ZnO	8.31±0.25	0.19±0.01	0.60±0.08	1.00
LDPE 18 % ZnO	8.31±0.52	0.21±0.02	0.50±0.05	1.04
LDPE 24 % ZnO	7.90±0.62	0.22±0.02	0.41±0.11	1.11
LDPE 36 % ZnO	7.86±0.49	0.24±0.02	0.16±0.04	1.24

4. Conclusion

This study involves the investigation of electrical, thermal and morphological properties of the prepared LDPE/ZnO films. The thermal stability of the LDPE increased with the presence of the ZnO nano particles, and it was seen that the degradation temperatures of the nanocomposites showed an increase with increasing content of the ZnO in the nanocomposites. ZnO particle addition changed the tensile strength of the nanocomposite slightly while elastic modulus increased from 0.13 GPa (pure LDPE,) to 0.24 GPa (36 wt% ZnO). On the other hand, elongation of the nanocomposites decreased apparently due to increment in stiffness of the polymer with the addition of ZnO. The dielectric constant $\varepsilon'(\omega)$ and the dielectric loss $\varepsilon''(\omega)$ of the nanocomposite films were found to decrease with increasing frequency. It was observed that the addition of nano-sized ZnO filler leaded to the formation of polymer/ZnO interface, which improved the dielectric function. The study indicates that the good dispersions of ZnO nanoparticles in LDPE polymer matrix, up to 12 wt%, can be achieved without using compatibilizers. This also indicates the improvements on the electrical properties of the nanocomposites can be controlled with the amount and dispersion of the incorporated ZnO nano particles. As a result, it can be say that the LDPE/ZnO nanocomposite films have the potential to use in electrical devices for various applications due to their improved electrical properties.

References

[1] A. C. Balazs, T. Emrick, T. P. Russell, Science **314**, 1107 (2006).

[2] Y. Lin, A. Boker, J. B. He, K. Sill, H. Q. Xiang, C. Abetz, et al., Nature 434, **55** (2005).

[3] R. F. Gibson, Compos. Struct. **92**, 2793 (2010).

[4] M. Jouni, A. Boudenne, G. Boiteux, V. Massardier, B. Garnier, A. Serghei, Polym. Compos. **34**, 778 (2013).

[5] A. Ballestar, F. Yakuphanoglu, B. F. Senkal, M. Munoz, W. A. Farooq, Optoelectron. Adv. Mat. **5**, 177 (2011).

[6] M. P. Ajayan, L. S. Schadler, P. V. Braun, Nanocomposite Science and Technology, John Wiley&Sons 77 (2003).

[7] Y. Pan, X. Liu, X. Hao, Z. Stary, D. W. Schubert, E Polym J. **78**, 106 (2016).

[8] K. R. Reddy, B. C. Sin, K. S. Ryu, J. Noh, Y. Lee, Synthetic Met. **159**, 1934 (2009).

[9] K. R. Reddy, K. P. Lee, A. I. Gopalan, Colloid. Surface. A **320**, 49 (2008).

[10] M. Hassan, K. R. Reddy, E. Haque, S. N. Faisal, S. Ghasemi, A. I. Minett, V. G. Gomes, Compos. Sci. Tech. **98**, 1 (2014).

[11] M. Ghislandi, E. Tkalya, A. Alekseev, C. E. Koning, G. De With, Appl. Maters Today **1**, 88 (2015).

[12] L. Xu, G. Chen, W. Wang, L. Li, X. Fang, Compos. Part A **84**, 472 (2016).

[13] Z. Dang, L. Fan, S. Zhao, C. Nan, Mater. Res. Bull. **38**, 499 (2003).

[14] C. K. Huang, S. W. Chen, W. C. J. Wie, J. Appl. Polym. Sci. **102**, 6009 (2006).

[15] A. Somwangthanaroj, C. Phanthawonge, S. Ando, W. Tanthapanichakoon, J. Appl. Polym. Sci. **110**, 1921 (2008).

[16] A. Moezzi, A. M. McDonagh, M. B. Cortie, Chem. Eng. J. **185**, 1 (2012).

[17] S. J. Pearton, D. P. Norton, K. Ip, Y.W. Heo, T. Steiner, Prog. Mater. Sci. **50**, 293 (2005).

[18] M. G. Nair, K. R. Nirmala, K. Rekha, et al., Mater. Lett. **65**, 1797 (2011).

[19] X. Y. Ma, W. D. Zhang, Polym. Degrad. Stabil. **94**, 1103 (2009).

[20] M. S. Cao, W. L. Song, W. Zhou, D. W. Wang, J. L. Rong, et al., Compos. Struct. **92**, 2984 (2010).

[21] W. Zhang, X. Chen, N. Xu, R. Xiang, Y. Zhu, Z. Tang, J. Nanomater. doi:10.1155/2013/986157 (2013).

[22] Y. W. Chen, Y. C. Liu, S. X. Lu, C. S. Xu, C. L. Shao, C. Wang, et al., J. Chem. Phys. **123**, 134701 (2005).

[23] Y. Zhang, H. B. Jia, X. H. Luo, X. H. Chen, D. P. Yu, R. M. Wang, J. Phys. Chem. B **107**, 8289 (2003).

[24] S. J. Chen, Y. C. Liu, C. L. Shao, R. Mu, Y. M. Lu, J. Y. Zhang, et al., Adv. Mater. **17**, 586 (2005).

[25] D. Sun, N. Miyatake, H. J. Sue, Nanotechnology **18,** 215606 (2007).

[26] M. S. Gaur, P. K. Singh, R. S. Chauhan, J. Appl. Polym. Sci. **118**, 2833 (2010).
[27] S. C. Tjong, G. D. Liang, Mater. Chem. Phys. **100**, 1 (2006).
[28] S. K. Esthappan, A. B. Nair, R. Joseph, Composites B **69**, 145 (2015).
[29] H. Wu, C. Lu, W. Zhang, X. Zhang, Mater. Design. **52**, 621 (2013).
[30] A. S. Luyt, J. A. Molefi, H. Krump, Polym. Degrad. Stabil. **91**, 1629 (2006).
[31] H. H. Redhwi, M. N. Siddiqui, A. L. Andrady, S. Hussain, J. Nanomater. **2013**, 1 (2013).
[32] X. Huang, P. Jiang, C. Kim, Q. Ke, G. Wang, Compos. Sci. Tech. **68**, 2134 (2008).
[33] J. I. Hong, P. Winberg, L. S. Schadler, R. W. Siegel, Mater. Lett. **59**, 473 (2005).
[34] F. Tian, Q. Lei, X. Wang, Y. Wang, IEEE. T. Dielect. El. In. **19**, 763 (2012).
[35] Z. Dang, L. Fan, Y. Shen, C. W. Nan, S. Zhao, J. Therm. Anal. Calorim. **71**, 635 (2003).
[36] H. Wang, G. Xie, C. Yang, Y. Zheng, Z. Ying, W. Ren, Y. Zeng, Polym. Compos. doi: 10.1002/pc.23569 (2015).
[37] Z. H. Dang, Y. H. Zhang, S. C. Tjong, Synthetic Met. **146**, 79 (2004).
[38] S. Z. Cheng, Handbook of Thermal Analysis and Calorimetry: Applications to Polymers and Plastics, Elsevier (2002).
[39] B. Wunderlich, Macromolecular Physics II., Academic Press, New York (1973).
[40] X. Jiang, L. T. Drzal, Polym. Compos. **33**, 636 (2012).
[41] P. Rizzo, F. Baione, G. Guerra, L. Martinotto, E. Albizzati, Macromolecules **34**, 175 (2001).
[42] H. Zhao, R. K. Y. Li, Polymer **47**, 3207 (2006).
[43] A. K. Jonscher, Nature **267**, 673 (1977).
[44] R. Macdonald, Impedance Spectroscopy, Theory, Experiment, and Applications, John Wiley & Sons (2005).
[45] C. G. Koops, Phys. Rev. **83**, 121 (1951).
[46] Z. Dang, L. Fan, S. Zhao, C. Nan, Mater. Sci. Eng. B **99**, 386 (2003).
[47] M.B. Heaney, Phys. Rev. B **52,** 12477 (1995).
[48] Y. Rao, J. Qu, T. Marinis, C. P. Wong, IEEE Trans. Compon. Packag. Technol. **23**, 680 (2000).
[49] Z.-M. Dang, L.-Z. Fan, Y. Shen, C.-W. Nan, Chem. Phys. Lett. **369,** 95 (2003).
[50] A. K. Mishra, S. Ramaprabhu, Chem. Eng. J **187**, 10 (2013).
[51] F. Henry, P. Marchal, J. Bouillard, A. Vignes, O. Dufaud, L. Perrin, Chem. Eng. Trans. **31**, 811 (2013).

*Corresponding author: hberber@yildiz.edu.tr